Rotational bands in the quadrupole-octupole collective model

A. Dobrowolski,[1,*] K. Mazurek,[2,†] and A. Góźdź[1,‡]
[1]*Department of Theoretical Physics, Maria Curie-Skłodowska University, pl. Marii Curie-Skłodowskiej 1, PL-20031 Lublin, Poland*
[2]*Institute of Nuclear Physics PAN, ul. Radzikowskiego 152, Pl-31342 Kraków, Poland*

(Received 16 November 2017; revised manuscript received 16 January 2018; published 16 February 2018)

A collective band of positive as well as negative parity could be composed of vibrational and rotational motions. The octupole vibrational configurations can be based either on axial or nonaxial octupole excitations. A consistent approach to the quadrupole-octupole collective vibrations coupled with the rotational motion enables us to distinguish between various scenarios of disappearance of the $E2$ transitions in negative-parity bands observed in several nuclei. The theoretical estimates presented here are compared with the very recent experimental energies and transition probabilities in and between the ground-state and low-energy negative-parity bands in ^{156}Dy. A realistic collective Hamiltonian contains the potential-energy term obtained through the macroscopic-microscopic Strutinsky-like method with a particle-number-projected BCS approach and a deformation-dependent mass tensor. The potential energy and the inertia parameters are defined in the vibrational-rotational, nine-dimensional collective space of the multipole-deformation parameters and Euler angles. The symmetrization procedure applied to the eigenstates of the collective Hamiltonian ensures their uniqueness with respect to the laboratory coordinate system. This quadrupole-octupole collective approach may also allow us to find and/or verify some fingerprints of possible high-rank symmetries (e.g., tetrahedral, octahedral, ...) in nuclear collective bands.

DOI: 10.1103/PhysRevC.97.024321

I. INTRODUCTION

The idea of looking for the experimental evidence of the high-rank symmetries in atomic nuclei has been triggered by a series of theoretical articles (see, e.g., Refs. [1–5]), where existence of the nonaxial octupole stable configurations have been connected with negative-parity bands. The octupole deformation of the nucleus was confirmed experimentally by studies of experimental observables such as rotational spectra of quadrupole or octupole deformed nuclei [6,7], the transition probabilities, magnetic moments and some properties of K isomers [8,9]. Recently, the investigation of negative-parity, odd-spin states in ^{156}Dy has been repeated with the high-resolving power of the Gammasphere array [10].

The most expected evidence of the nonaxial octupole deformation of rotating nucleus would be the disappearance of the $E2$ transitions between the lowest states in the negative-parity band. The $E2$ transitions are measured in "band 2" (odd spin) and "band 4" (even spin) of Ref. [10] for ^{156}Dy. In band 2, the $E2$ transitions are measured starting from the state 27^- down to 7^-. Reference [10] presents also two other negative-parity bands exhibiting the rotational structure ("band 5" and "band 6"), starting from spin 7^- up, but they have been measured in older experiments, where only the energy spectra have been accessible. Since for these two bands there are neither the values of the reduced transition probabilities nor any branching ratios, we are not able to reliably judge their intrinsic structure in the current study. Thus the main attention will be focused on bands 2 and 4.

Since in our previous work of Ref. [11] the ground-state and the negative-parity odd-spin bands for ^{156}Gd nucleus was discussed in the collective quadrupole-octupole model in the low-spin regime ($0 < J < 5$), we now want to extend the study to somewhat higher spins. Our approach describes the rotational-vibrational character of the spectra but it does not take into account any microscopic properties, e.g., particle-hole excitations. We hope that we will also be able to, at least, partly answer the question posed by the authors of Ref. [10] in Sec. IV B concerning the band 2 and/or band 4: *octupole vibrations or tetrahedral symmetry?*

Nuclear vibrations have been discussed by several authors in Refs. [12,13] by using the Bohr–Hamiltonian model [14,15] or by the interacting boson model (IBM) [16] or the analytic collective model (AQOA) [17]. Also the new approach based on the cluster Hamiltonian is shown in Ref. [18]. All these approaches are aimed at searching for stable nuclear configurations and the strengths of the electromagnetic transitions between collective states, where quadrupole and octupole deformation parameters play the role of dynamical collective variables.

The collective Hamiltonian used in the present investigation contains the collective potential obtained within the macroscopic-microscopic calculations using the Strutinsky method with the Woods–Saxon mean field [3,19]. The mass tensors and moments of inertia in the kinematic part are given by the cranking approximation [20]. The vibrational-rotational Hamiltonian is constructed in the intrinsic frame by

*arturd@kft.umcs.lublin.pl
†katarzyna.mazurek@ifj.edu.pl
‡andrzej.gozdz@umcs.lublin.pl

applying the so-called *adiabatic approximation*. The spherical harmonics parametrization of the nuclear deformation allow us to control the geometrical properties of the nuclear surface and apply the *symmetrization procedure*. The deformation space is limited to the "induced" dipole ($\lambda = 1$), quadrupole ($\lambda = 2$), and octupole ($\lambda = 3$) multipole deformation parameters.

The collective Hamiltonian is diagonalized in the space of the symmetrized basis functions. In a final step, for a selected Hamiltonian, eigenstates identified as the members of band 2, band 4, and ground-state bands, the reduced probabilities of electric interband dipole and intraband quadrupole transitions are calculated. More details of this approach are presented in Ref. [11]. The accompanying problem of the center-of-mass shift has also been discussed in Ref. [21]. We want to stress that, in fact, in the calculations we generate negative-parity one-phonon-model bands based on all four $\alpha_{3\nu}$ octupole excitations with even and odd spins up to $J = 9$. Next, the energetic and reduced-transition properties of all these model bands are confronted with either experimental band 2 or band 4 to choose the most suitable theoretical candidates. As a matter of fact, the reduced-transition properties of all proposed odd-spin bands do not differ from each other as dramatically as in the case of even-spin model bands. For the even-spin sequence of band 4 we have found only the one theoretical candidate, having $B(E2)/B(E1) \approx 20$ (experimentally around 150), where the interband $B(E2)$ values are expressed in hundreds Weisskopf units. For the remaining even-spin theoretical sequences with $B(E2)$ values given in tens of W.u. and many order-of-magnitude-lower $B(E1)$ values, these ratios are 2–8 orders of magnitude higher; thus we give up to display them here.

An interesting outcome of this study is the fact that each state belonging to a given vibrational-rotational band; in particular band 2 and band 4, contains the superposition of the rotational contributions with different K quantum numbers in uncorrelated percentage. As usually, K stands for the projection of the angular momentum on the chosen quantization axis of the intrinsic reference system.

The paper is organized as follows: Section II gives the details of the collective quadrupole-octupole model and the problem of uniqueness of intrinsic vibrational-rotational Hamiltonian eigensolutions in the laboratory frame. Section III is devoted to the properties of the negative-parity model bands. The theoretical transition energies and branching ratios are compared with experimental data. The article is closed with the summary.

II. COLLECTIVE QUADRUPOLE-OCTUPOLE MODEL

The vibrational-rotational collective bands of positive or negative parity can be modeled with the use of either even or odd-multipolarity $\alpha_{\lambda\mu}$ deformations, where $\lambda = 1, 2, 3, \ldots$ and $\mu = -\lambda, -\lambda+1, \ldots, +\lambda$. In the following applications these deformation parameters become the dynamical collective variables describing surface vibrations in the intrinsic frame. The variables $\alpha_{\lambda\mu}$ are also the spherical components of the irreducible tensor with respect to the SO(3) group, so their properties are well defined with regard to the group theory formalism.

The nuclear surface is expanded in the body-fixed reference frame in terms of the orthogonal basis set of the spherical harmonics $\{Y_{\lambda\mu}\}$. As shown in Ref. [11], the dipole α_{10} and $\alpha_{1\pm1}$ variables are determined from the condition that the center of mass of the nuclear body is fixed in the beginning of the coordinate system.

The space spanned by two quadrupole variables, α_{20}, $\alpha_{22} = \alpha_{2\text{-}2}$ with the conditions $\alpha_{21} = \alpha_{2\text{-}1} = 0$ defines the body-fixed frame and Euler angles of the discussed model. Therefore, this set together with the full octupole $\{\alpha_{3\nu}\}, \nu = 0, \pm1, \pm2, \pm3$ complex tensor and three Euler angles Ω form the twelve-dimensional collective space. However, fixed in this way, the intrinsic frame is not the principal-axis frame of the quadrupole-octupole body but it permits us to use the traditional picture of the collective quadrupole motion, where, at least, the quadrupole $Q_{2\mu}$ tensor is diagonal, extended by the presence of independent octupole vibrations. The calculation of the matrix elements of the collective Hamiltonian and/or any physical observables with a satisfactory accuracy is a serious task in a so-defined multidimensional space.

A further limitation of the $\{\alpha_{3\nu}\}$ values to *real* numbers implies that $\alpha_{3\mu}$ and $\alpha_{3\text{-}\mu}$ become mutually dependent. Obtained in such a way, the reduction of the collective-space dimensionality to nine dimensions (including Euler angles) allows now for an efficient determination of the time-consuming multidimensional integrals and, consequently, an investigation of contributions from individual collective modes. The use of the so-called *adiabatic approximation* allows the vibrational and rotational matrix elements of the Hamiltonian to be calculated separately. Moreover, the rotational matrix elements depending only on the Euler angles may be calculated analytically.

Actually, the independent vibrational collective variables of the present approach are $(\alpha_{20},\alpha_{22},\{\mathrm{Re}(\alpha_{3\nu})\})$ with ν being index running over non-negative integers only, i.e., $\nu = 0,1,2,3$, describing the axial and nonaxial quadrupole vibrational modes and four real octupole modes, respectively. With the above, the nuclear surface as function of (ϑ,φ) angles can be expressed in the body-fixed frame as

$$R(\vartheta,\varphi) = R_0 c(\alpha)\Big\{1 + \alpha_{10}Y_{10}(\vartheta,\varphi) + \alpha_{20}Y_{20}(\vartheta,\varphi) + 2\alpha_{11}\mathrm{Re}[Y_{11}(\vartheta,\varphi)] + 2\alpha_{22}\mathrm{Re}[Y_{22}(\vartheta,\varphi)] + \alpha_{30}Y_{30}(\vartheta,\varphi) + 2\sum_{\mu=1}^{3}\alpha_{3\mu}\mathrm{Re}[Y_{3\mu}(\vartheta,\varphi)]\Big\}, \quad (1)$$

where the function $c(\alpha)$ ensures the volume conservation of the deformed body.

The angles (ϑ,φ) measured with respect to the intrinsic frame parametrize the points on the nuclear surface. These angles do not belong to the set of the collective variables. The orientation of the nuclear surface with respect to the laboratory frame is described by the Euler angles $\Omega = (\Omega_1,\Omega_2,\Omega_3)$, which are treated here as collective degrees of freedom in the intrinsic frame.

The problem of the center-of-mass shift as a result of the presence of the mass asymmetry in octupole-deformed nuclei is widely discussed in Refs. [11,21].

For fixed values of the quadrupole deformations $(\alpha_{20},\alpha_{22})$, the conditions $\mathrm{Im}(\alpha_{3\mu}) = 0$ imposed on the intrinsic $\alpha_{3\mu}$ tensor mean that a single octupole shape can be obtained with more than one set $(\alpha_{30},\alpha_{31},\alpha_{32},\alpha_{33})$. Generated in this way, shapes have, however, different orientations with respect to the axes of the laboratory frame. To avoid the nonuniquenesses of the wave functions in the laboratory frame caused by the above limitations on the collective space along with the conditions to define the intrinsic frame, one has to introduce the *symmetrization* procedure.

Briefly, each physical state which describes the system in the laboratory frame should necessarily be invariant with respect to the so-called symmetrization group $\bar{G}_s$, acting within the intrinsic frame. Such a group should always be determined individually, depending on the set of $\alpha_{\lambda\mu}$ variables involved in the model. For present octupole variables, the symmetrization group is $\bar{G}_s = \bar{D}_{4y}$ and it is lower than the octahedral group in a pure quadrupole Bohr–Hamiltonian model. Its elements (rotations) $\bar{g}$ are $(I, C_{2x}, C_{2y}, C_{2z}, C_{4y}, C_{4y}^{-1}, C_{2c}, C_{2d})$, where C_{ni} (for $i = \{x,y,z\}$) denote the rotations about $2\pi/n$ angle around the ith axis, including some skew to the OX, OY, and OZ axes. Finally, for all $\bar{g} \in \bar{G}_s$, the symmetrization condition applied to any collective state $\Psi(\alpha,\Omega)$ reads

$$\bar{g}\Psi(\alpha,\Omega) = \Psi(\alpha,\Omega). \tag{2}$$

The relation (2) ensures the uniqueness of the Hamiltonian eigensolutions in the laboratory frame. In the context of the Hamiltonian-symmetry problem, the symmetrization group $\bar{G}_s$ can be treated as its *minimal* symmetry group. This implies that both the kinetic and potential components of the full Hamiltonian exploited in this study have to be, at least, $\bar{G}_s$ invariant.

A. Collective Hamiltonian

Habitually, a consistent vibrational-rotational collective approach is constructed by defining the Hamiltonian with respect to the laboratory frame, spanned by the laboratory collective variables. In the next step, this Hamiltonian is transformed to the body-fixed frame. For the quadrupole collective space a standard kinetic-energy term obtained with this prescription results, e.g., with the well-known Bohr–Hamiltonian approach.

In contradiction to the above-outlined scheme, the used here of the collective vibrational-rotational Hamiltonian is already written in the intrinsic frame. The already-mentioned adiabatic approximation is introduced in order to separate the vibrational and rotational motions. In principle, such separation is possible due to the difference of typical energy scales for both of these modes. Furthermore, quadrupole and octupole vibrational modes are assumed to be totally decoupled in the kinetic-energy term. As easily deduced, this accelerates numerical calculations by a factor equal to the number of mesh points of the quadrupole subspace $\{\alpha_{20},\alpha_{22}\}$, i.e., about 2×10^3.

Therefore, we calculate two independent mass tensors: first for pure quadrupole motion, where the octupole deformation corresponds to the potential-energy minimum with all $\alpha_{3\nu} = 0$, and the second describing pure octupole vibrations performed around the equilibrium shape.

This simplification leads to a quantized realistic quadrupole-octupole-vibrational Hamiltonian with deformation-dependent inertia parameters:

$$\begin{aligned}
&\hat{\mathcal{H}}_{\mathrm{coll}}(\alpha_2,\alpha_3,\Omega) \\
&= \frac{-\hbar^2}{2}\left\{\frac{1}{\sqrt{|B_2|}}\sum_{\nu\nu'=0}^{2}\frac{\partial}{\partial\alpha_{2\nu}}\sqrt{|B_2|}\left[B_2^{-1}\right]^{\nu\nu'}\frac{\partial}{\partial\alpha_{2\nu'}}\right. \\
&\quad\left.+\frac{1}{\sqrt{|B_3|}}\sum_{\mu\mu'=0}^{3}\frac{\partial}{\partial\alpha_{3\mu}}\sqrt{|B_3|}\left[B_3^{-1}\right]^{\mu\mu'}\frac{\partial}{\partial\alpha_{3\mu'}}\right\} \\
&\quad+\hat{H}_{\mathrm{rot}}(\Omega)+\hat{V}(\alpha_2,\alpha_3),
\end{aligned} \tag{3}$$

where α_2 and α_3 describe the subspaces of the quadrupole and octupole variables with metrics $B_2(\alpha_2)$, $B_3(\alpha_3)$ given in this approach as the quadrupole and octupole microscopic mass tensors, respectively. Quantities $|B_2| = \det(B_2(\alpha_2))$ and $|B_3| = \det(B_3(\alpha_3))$ stand for square roots of the metric-tensor determinants. Above, Ω denotes the set of three Euler angles describing relative orientations of the axes of the intrinsic versus laboratory frames. The microscopic mass tensors are determined via the *cranking* method of Ref. [20]. Its covariant component, $B_{\lambda\nu,\lambda\nu'}$, for $\lambda = 2$ or $\lambda = 3$ and indices $\nu > 0$ is given by the expression

$$B_{\lambda\nu,\lambda\nu'}(\{\alpha_{\lambda\mu}\}) = \sum_{kl}\frac{\langle\phi_k|\frac{\partial\hat{H}_{\mathrm{sp}}}{\partial\alpha_{\lambda\nu}}|\phi_l\rangle\langle\phi_l|\frac{\partial\hat{H}_{\mathrm{sp}}}{\partial\alpha_{\lambda\nu'}}|\phi_k\rangle}{(E_k+E_l)^3}(u_k v_l + v_k u_l)^2, \tag{4}$$

where the double sum runs over the full set of the BCS quasiparticle (including time-reversed) states, obtained out of eigensolutions of the mean-field Hamiltonian $\hat{H}_{\mathrm{sp}}$ used the and chosen pairing model. Quantities v_n are the occupation probability amplitudes of the nth quasiparticle state while u_n is given by the normalization relation $u_n^2 = 1 - v_n^2$. In the denominator of Eq. (4), E_k and E_l are the quasiparticle energies of kth and lth states.

In this work, contrary to nowadays-applied self-consistent methods, an effective approximation to generate the collective potential in the six-dimensional space of $\{\alpha_2,\alpha_3\}$ variables is still a widely applied macroscopic-microscopic model. This model, for a careful choice of the mean-field potential, pairing interaction, and smooth liquid-drop energy contribution, is able to produce reliable estimates of the potential-energy surfaces $\hat{V}(\alpha_{2\nu},\alpha_{3\mu})$. Within this study we use the Woods–Saxon potential [22] with the so-called *universal* parameters [19] (refitted to the newer data of Ref. [23]) which delivers single-particle energies and eigenstates for a desired mean-field deformation. Both of these quantities are "input" quantities for calculations of quantum shell and pairing energies as well as mass parameters through Eq. (4).

B. Rotational term

Due to significantly different energy regimes of the vibrational and rotational modes, they are here totally decoupled.

Hence, the rotational term $\hat{H}_{\rm rot}(\Omega)$ depends only on the Euler angles and, parametrically, on the static nuclear deformation, here corresponding to the equilibrium point. Since, as mentioned in Sec. II, the rotational Hamiltonian has to be invariant with respect to the symmetrization group $\bar{G}_s$, so we construct it by using irreducible (spherical) tensors of the SO(3) group, $\hat{\mathcal{T}}_{\lambda\mu}(n;\lambda_2=2,\lambda_3=3,\ldots,\lambda_{n-1}=(n-1))$, as done, e.g., in Refs. [11,24,25].

The rotor Hamiltonian $\hat{\mathcal{H}}_{\rm rot}$ of given symmetry $\bar{G}_s$ and multipolarity λ can be defined as the linear combination of $\hat{\mathcal{T}}$ with the condition that $n=\lambda$ and the constant term $T_{00}(n=2)$ as

$$\hat{\mathcal{H}}_{\rm rot}=\sum_{\lambda=0}^{\lambda_{\rm max}}\sum_{\mu=-\lambda}^{\lambda}c_{\lambda\mu}\hat{\mathcal{T}}_{\lambda\mu}+c_{00}T_{00}(n=2). \tag{5}$$

The upper limit of multipolarities $\lambda_{\rm max}$ is, in general, arbitrary. In this work we limit ourselves to $\lambda_{\rm max}=2$. The tensors $\hat{\mathcal{T}}_{\lambda\mu}(n;\lambda_2=2,\lambda_3=3,\ldots,\lambda_{n-1}=(n-1))$ entering Eq. (5) are constructed out of the spherical components of the angular-momentum operators in the following way:

$$\begin{aligned}&\hat{\mathcal{T}}_{\lambda\mu}(n;\lambda_2=2,\lambda_3=3,\ldots,\lambda_{n-1}=(n-1))\\&\quad\equiv\left[\left(\left(\left(\hat{J}\otimes\hat{J}\right)_{\lambda_2}\otimes\hat{J}\right)_{\lambda_3}\otimes\cdots\otimes\hat{J}\right)_{\lambda_{n-1}}\right]_{\lambda\mu},\end{aligned} \tag{6}$$

where n and λ are respectively the rank and multipolarity of the resulting tensor, and λ_k for $k=2,3,\ldots,n-1$ are the multipolarities of tensors arising in the intermediate coupling steps. The coupling of angular-momentum spherical tensors of multipolarity $\lambda=1$ in Eq. (6) is given within the standard way by using the SO(3) Clebsch–Gordan coefficients $(1,\mu;1,\mu'|\lambda_2\mu_2)$:

$$\left(\hat{J}\otimes\hat{J}\right)_{\lambda\mu}=\sum_{\mu=-1}^{1}\sum_{\mu'=-1}^{1}(1\mu1\mu'|\lambda\mu)\hat{J}_{1\mu}\hat{J}_{1\mu'}. \tag{7}$$

Let us notice that, constructed in such a way, the rotational Hamiltonian is coupled solely by the angular-momentum operators and does not contain explicit derivatives over the Euler angles. The latter indicates that no Coriolis interaction is simulated here.

The coupling constants c_{00}, c_{20}, and c_{22} in Eq. (5) can be expressed through the moments of inertia as

$$\begin{aligned}c_{00}&=-\frac{1}{\sqrt{12}}\left(\frac{1}{I_x}+\frac{1}{I_y}+\frac{1}{I_z}\right),\\c_{20}&=\frac{1}{\sqrt{6}}\left(\frac{1}{I_z}-\frac{1}{2I_x}-\frac{1}{2I_y}\right),\\c_{22}&=\frac{1}{4}\left(\frac{1}{I_x}-\frac{1}{I_y}\right),\end{aligned} \tag{8}$$

where I_x, I_y, and I_z are the microscopic nuclear moments of inertia with regard to Ox, Oy, and Oz axes, respectively, obtained also in the cranking approximation.

If the $\bar{D}_{4y}$-symmetric rotor Hamiltonian $\hat{H}_{\rm rot}(\Omega)$ of Eq. (3) is needed, the quadrupole coupling constants entering Eq. (5) fulfill the approximate relation $c_{22}\approx c_{20}/0.8165$.

Following the symmetrization idea, the basis in which the full collective Hamiltonian (3) is diagonalized contains functions symmetrized with respect to the intrinsic group $\bar{D}_{4y}$. Recall that the intrinsic group, by definition, acts in the intrinsic collective space containing Euler angles.

In numerical calculations it is very convenient to use the projection-operator formalism which defines the projection of an initial wave function onto the selected irreducible representation of the symmetry group. If one chooses, in particular, the scalar (A1) representation of the symmetrization $\bar{G}_s$ group, such a procedure is equivalent to the symmetrization condition (2).

Applying the explicit form of the projection operator $\hat{P}^{(A1)}$ on the six-dimensional "shifted" harmonic-oscillator solution combined with the appropriate Wigner function, one gets the nth symmetrized basis function as

$$\begin{aligned}\Psi^{(\pm)}_{n;JM\kappa}=\hat{P}^{(A1)}\Psi_{k;JMK\pi}=\frac{\sqrt{2J+1}}{8}\sum_{i=1}^{8}&u_{n_{20}}(\eta_{20},\hat{\bar{g}}_i\alpha_{20}-\mathring{\alpha}_{20})u_{n_{22}}(\sqrt{2}\eta_{22},\hat{\bar{g}}_i\alpha_{22}-\mathring{\alpha}_{22})u_{n_{30}}(\eta_{30},\pm\hat{\bar{g}}_i\alpha_{30}-\mathring{\alpha}_{30})\\&\times u_{n_{31}}(\sqrt{2}\eta_{31},\pm\hat{\bar{g}}_i\alpha_{31}-\mathring{\alpha}_{31})u_{n_{32}}(\sqrt{2}\eta_{32},\pm\hat{\bar{g}}_i\alpha_{32}-\mathring{\alpha}_{32})u_{n_{33}}(\sqrt{2}\eta_{33},\pm\hat{\bar{g}}_i\alpha_{33}-\mathring{\alpha}_{33})\sum_{K=-J}^{J}D^{\lambda}_{\kappa K}(g_i)D^{J\star}_{MK}(\Omega),\end{aligned} \tag{9}$$

where the set of all eight elements $\hat{\bar{g}}_i$ forms the symmetrization group. Parameters $\mathring{\alpha}_{2\nu}$ and $\mathring{\alpha}_{3\mu}$ describe the position of the potential-energy-well minimum. Studying potential-energy maps of Sec. II C, we can conclude in advance that $\mathring{\alpha}_{20}=0.25$, $\mathring{\alpha}_{22}=0$, and all $\mathring{\alpha}_{3\mu}=0$. Quantities $\eta_{\lambda\nu}$ set down as the widths of individual functions $u_m(\eta,\mathring{\alpha};\alpha)$ are assumed to be the normalized, one-dimensional m-phonon harmonic-oscillator solutions. The determination of the η-like parameters is outlined in Sec. III C.

The basis states of the positive (+) or negative (−) parity are obtained as the linear combinations of functions (9), $\frac{1}{2}[\Psi^{(+)}_{n;JM\kappa}+\Psi^{(-)}_{n;JM\kappa}]$ and $\frac{1}{2}[\Psi^{(+)}_{n;JM\kappa}-\Psi^{(-)}_{n;JM\kappa}]$, respectively.

C. Collective potential

As already mentioned, the estimates of the total potential energy of the deformed nucleus are obtained within the phenomenological mean-field approach, known as the macroscopic-microscopic method of Strutinsky. In this method, as commonly known, the macroscopic energy term given usually by the liquid-drop-type formula is modified

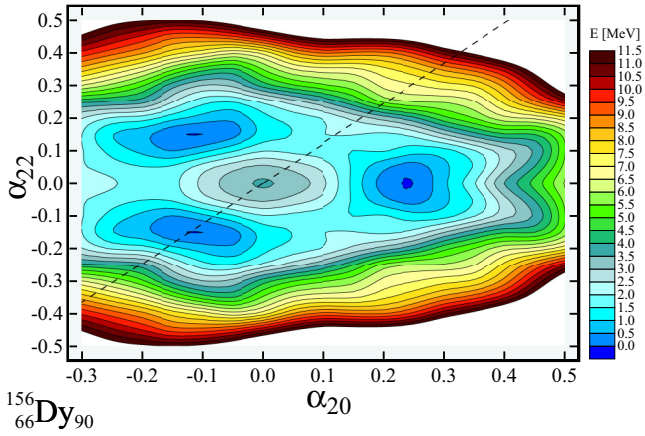

FIG. 1. The potential energy of ^{156}Dy in the quadrupole plane (α_{20},α_{22}).

by the microscopic shell- and pairing-energy corrections, describing quantum effects in a nucleus. However, this kind of approach has been applied for more than five decades now and is still a powerful and successful method, well suited particularly to large-scale calculations and able to produce results close to the experimental data. The details of this kind of calculation and the corresponding results are presented, e.g., in Refs. [26,27] and references therein.

The geometry of the potential-energy surfaces in the vicinity of the equilibrium state of cold, medium-mass nuclei generated, for example, by the Lublin–Strasbourg drop model (LSD) [28] is very similar to this, obtained from other competitive macroscopic models. Moreover, the LSD approach permits us to successfully reproduce fission barriers of actinides; see, e.g., Ref. [29].

The microscopic-energy correction is defined as the sum of the shell- and pairing-energy corrections to the smoothly changing liquid-drop energy.

The shell-energy correction arising due to the shell structure of a nuclear system is calculated by using the standard Strutinsky approach of the 6th order [30]. For the pairing energy [31,32], because of the difference between the sum of the single-particle energies and the energy of the pair correlations [33], the particle-number projected (PNP) pairing model within the standard BCS framework is applied.

The numerical calculations of the total collective potential entering Eq. (3) are performed in the six-dimensional mesh of vibrational collective variables: $\{\alpha_{20},\alpha_{22},\alpha_{3\nu},\nu = 0,1,2,3\}$ for the ^{156}Dy nucleus.

The ranges of nuclear deformation parameters as well as the corresponding mesh steps $\Delta\alpha_{\lambda\mu}$ are listed below:

$$\begin{aligned} &\alpha_{2\nu}\epsilon(-1.0;1.0), \quad \Delta\alpha_{2\nu} = 0.05, \quad \nu = 0,2, \\ &\alpha_{3\mu}\epsilon(-0.3;0.3), \quad \Delta\alpha_{3\mu} = 0.1, \quad \mu = 0,1,2,3, \end{aligned} \tag{10}$$

which gives a mesh of about two million points, describing various quadrupole-octupole nuclear shapes.

Figure 1 displays the total-energy map as function of the quadrupole (α_{20},α_{22}), putting the other four deformation parameters to zero. The equilibrium energy minimum corresponding to the quadrupole axial (prolate) shape of ^{156}Dy is visible. The straight dashed line of Fig. 1 on the (α_{20},α_{22}) cross section separates the quadrupole configurations, which are identical with respect to the $\bar{D}_{4y}$ symmetrization group. We clearly observe the ground-state energy occurring in the three (α_{20},α_{22}) quadrupole configurations.

The problem of the "repeatability" of the nuclear shapes as a results of the symmetrization with respect to the octahedral and $\bar{D}_{4y}$ groups is widely discussed in Ref. [11] and references therein. Now we want to recall that, in particular, the resulting Strutinsky potential energy as a function of the quadrupole and octupole deformation is invariant with regard to the symmetrization group $\bar{G}_s$. This property is true since the macroscopic liquid-drop contribution, as well as the microscopic shell- and pairing-energy corrections, depend only on the shape of the nuclear surface defined by Eq. (1). This means that, for a fixed quadrupole deformation, a single octupole shape for all $\alpha_{3\mu}^{(0)} \neq 0$ can be obtained by using eight different deformation-parameter combinations.

In general, the identical quadrupole-octupole shape for the $\bar{D}_{4y}$ symmetrization group is expected to show up, at a maximum, $2 \times 8 = 16$ times in the full (α_2,α_3) space. Otherwise, if it happens that all $\alpha_{3\mu}^{(0)} = 0$, such a shape appears, in fact, three times. Please recall that, in this particular case, the true symmetrization group is the octahedral, not $\bar{D}_{4y}$, group.

The dependence of the total potential energy on the quadrupole α_{20} and octupole $\alpha_{3\mu}$ degrees of freedom is shown in Fig. 2. Projections of the full potential-energy surface (PES) into axial quadrupole and selected octupole deformation parameter space permit us to trace the features of the global and local energy minima, such as their positions and depths.

The total-energy maps projected onto the (α_{20}, $\alpha_{3\mu}$) plane show two subtly pronounced identical minima for $\alpha_{20} < 0$ and $\alpha_{22} = 0$. Figure 2 shows that the ground-state well, which appears for octupoles $\alpha_{3\nu} = 0$, is the only stable configuration for the ^{156}Dy nucleus. Thus, the above-written arguments lead to the conclusion that one should obtain exactly two additional "copies" of this minimum, both again for $\alpha_{3\nu} = 0$. In Fig. 1, these minima are visible for α_{20} slightly below zero and $\alpha_{22} = 0$.

III. RESULTS

The model discussed here offers the positive- and negative-parity collective vibrational-rotational states based on $\alpha_{2\mu}$ and $\alpha_{3\nu}$ one-phonon excitations. On the basis of these states the reduced probabilities of the electric-dipole and quadrupole transitions are calculated and confronted with selected experimental results of Ref. [10].

A. Negative-parity bands

The negative-parity states are created in the potential-energy well based on the quadrupole-deformed ground-state configuration with quadrupole deformation $\alpha_{20} = 0.25$ and $\alpha_{22} = 0.0$. By consequence, the resulting octupole negative-parity states have a significant static quadrupole deformation producing large $B(E2)$ intraband transition probabilities. As deduced from the potential-energy plots of Fig. 2, the octupole

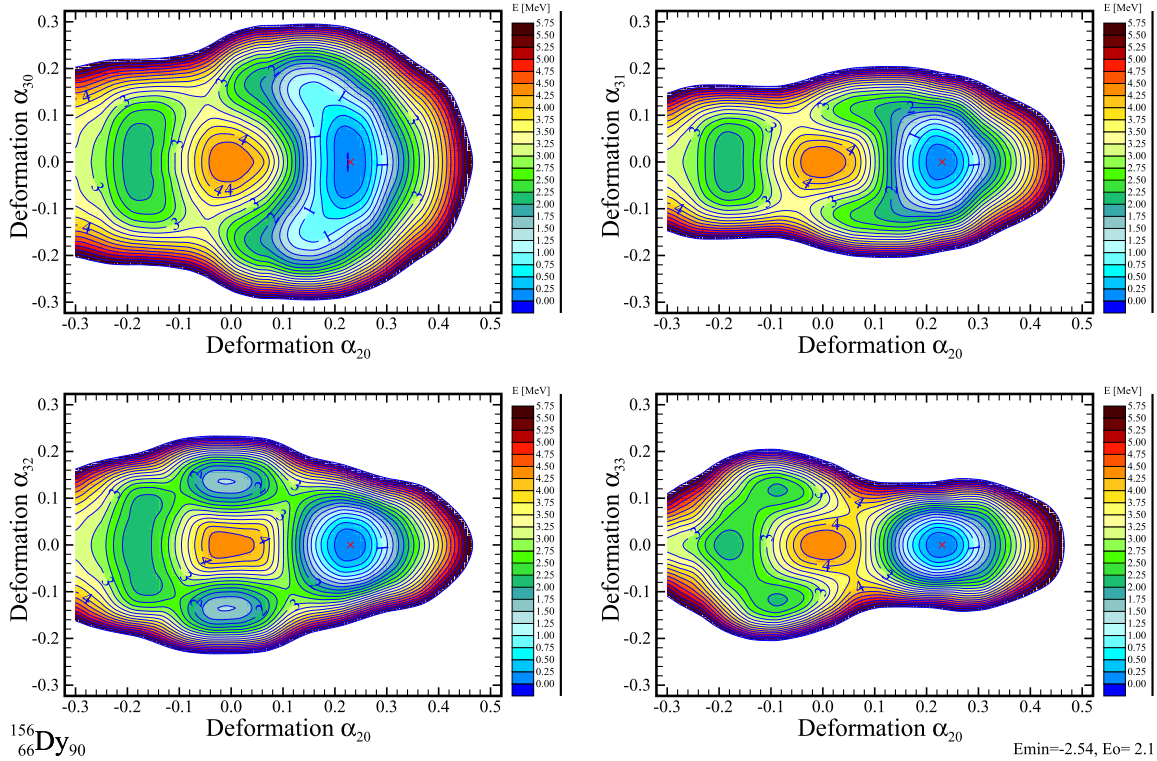

FIG. 2. Potential-energy maps generated for quadrupole (α_{20},$\alpha_{22}=0$) versus octupole (α_{30}, α_{31}, α_{32}, α_{33}) deformations.

vibrations (with multipolarity $\lambda = 3$) are performed around pure quadrupole shapes. In other words, the ^{156}Dy nucleus seems to have no stable configuration for which, at least, one of the static octupole deformations $\mathring{\alpha}_{3\nu} \neq 0$, $\nu = 0,1,2,3$.

As seen in Fig. 3, the odd-spin negative-parity bands, having as the bandhead axial α_{30} and nonaxial α_{31} one-phonon vibrational excitations, are shifted from each other in energy by about 70 keV whereas the band built on the tetrahedral α_{32} phonon lies higher by approximately 150 keV. The band built by the α_{33} one-phonon vibration is too high in energy compared with the previous three model bands, so is not considered in this study.

Due to the proximity in energy of the three of all four octupole bands mentioned, the photon energies of the dipole

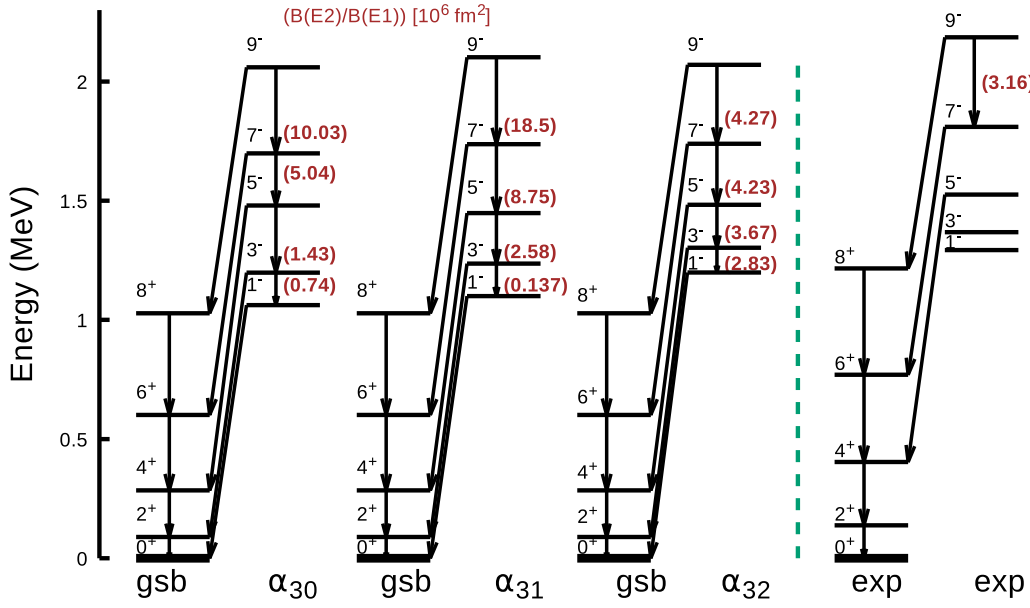

FIG. 3. The predicted ground-state and odd-spin negative-parity bands of ^{156}Dy. Arrows mark the $E1$ and $E2$ transitions. The branching ratios $B(E2)/B(E1)$ are written in parentheses.

TABLE I. γ-ray energies $E_\gamma^{\alpha_{30}}$, $E_\gamma^{\alpha_{31}}$, $E_\gamma^{\alpha_{32}}$, and $E_\gamma^{\alpha_{33}}$ predicted theoretically for all four model bands characterized by the type of octupole one-phonon excitation versus experimental results E_γ^{expt} measured at Gammasphere on ^{156}Dy [10].

Transition	$E_\gamma^{\alpha_{30}}$ keV	$E_\gamma^{\alpha_{31}}$ keV	$E_\gamma^{\alpha_{32}}$ keV	$E_\gamma^{\alpha_{33}}$ keV	E_γ^{expt} keV
$(3^- \to 1^-)$	136	136	104	104	
$(5^- \to 3^-)$	212	212	180	180	
$(7^- \to 5^-)$	289	289	247	152	
$(9^- \to 7^-)$	361	365	331	327	376
$(5^- \to 4^+)$	1115	1153	1188	1621	1121
$(5^- \to 6^+)$	809	847	882	1315	755
$(7^- \to 6^+)$	1098	1136	1138	1577	1039
$(7^- \to 8^+)$	671	709	711	1150	594
$(9^- \to 8^+)$	1032	1074	1042	1477	971
$(6^- \to 4^-)$	230		240	240	271
$(8^- \to 6^-)$	310		310	310	363
$(4^- \to 4^+)$	1080		1380	1810	1223
$(6^- \to 6^+)$	880		1020	1450	1128
$(8^- \to 8^+)$	760		900	1330	1046

interband transitions, $E_\gamma(\lambda = 1)$ (Table I), vary within an interval ± 0.1 MeV which is even less than the typical order of discrepancy between experimental results and theoretical predictions in up-to-date models.

In turn, the even-spin negative-parity band, marked in Ref. [10] as band 4, is shown in Fig. 4. The comparison with the calculated transition probability $B(E2)/B(E1)$ ratios and level energies allow us to ascribe this band to a "tetrahedral band," i.e., built on top of the one-phonon α_{32} excitation. In the case of the other vibrational modes, such as α_{30}, we obtain a $B(E2)/B(E1)$ ratio about two orders of magnitude too low or 2–8 orders of magnitude too high (for remaining nonaxial modes) in comparison with experimental data of Table II.

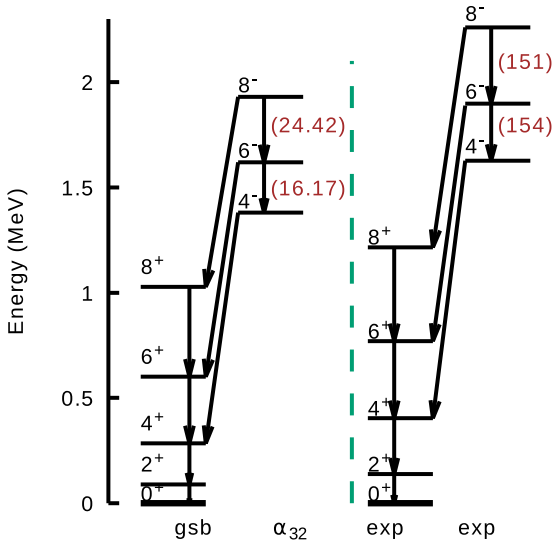

FIG. 4. Similar to Fig. 3 but for the predicted ground-state and even-spin negative-parity bands of ^{156}Dy.

TABLE II. Predicted intraband $E2$ and interband $E1$ transition probabilities for odd- and even-spin negative-parity and ground-state bands. Columns 2–5 correspond to negative-parity bands based on a given octupole $\alpha_{3\nu}$ excitation in ^{156}Dy.

Transition	$B(E2)$ [W.u.]			
$I_i^\pi \to I_j^\pi$	α_{30}	α_{31}	α_{32}	α_{33}
$3^- \to 1^-$	166	20	276	274
$5^- \to 3^-$	140	138	412	406
$7^- \to 5^-$	238	236	476	468
$9^- \to 7^-$	308	306	512	504
$6^- \to 4^-$	302		298	294
$8^- \to 6^-$	376		370	366
	$B(E1)$ [W.u.]			
	α_{30}	α_{31}	α_{32}	α_{33}
$3^- \to 2^+$	6.0×10^{-3}	3.8×10^{-3}	2.6×10^{-3}	1.2×10^{-4}
$5^- \to 4^+$	2.6×10^{-3}	1.4×10^{-3}	3.0×10^{-3}	2.0×10^{-4}
$7^- \to 6^+$	1.3×10^{-3}	7.2×10^{-4}	3.0×10^{-3}	1.4×10^{-4}
$9^- \to 8^+$	8.2×10^{-4}	4.4×10^{-4}	3.2×10^{-3}	2.2×10^{-4}
$6^- \to 6^+$	1.9×10^{-2}		0.5×10^{-3}	0.8×10^{-6}
$8^- \to 8^+$	1.6×10^{-2}		0.4×10^{-3}	2.7×10^{-6}

In the even-spin sequence, the mode α_{31} is expelled by the symmetrization procedure.

Looking only at the $E_\gamma^{\alpha_{30}}$ values of Table I, one is not able to reliably indicate at this stage which of these odd-spin negative-parity bands is the best candidate to reproduce the experimental collective bands referred to in Ref. [10] as band 2. However, for band 4, the tetrahedral mode seems to be preferable.

In the following section III C we come to the discussion of the reduced transition probabilities obtained [more precisely, the $B(E2)/B(E1)$ ratios] with the comparison with the measured values in these bands.

B. Rotational properties of states

As turns out, each vibrational-rotational negative-parity state of given spin J (in this work, $0 \leqslant J \leqslant 9$), characterized by a given type of octupole excitation and the number of excited phonons (here 1 or 3), can occur, e.g., for odd spin, in $(J+1)/2$ configurations, as shown in Fig. 5. They are described by specific combinations of rotational basis functions given as complex-conjugated Wigner functions $D^{J\star}_{MK}(\Omega)$ characterized in the intrinsic frame by a given K number and arbitrary M. These combinations, labeled here by κ $(-J \leqslant \kappa \leqslant J)$, are fixed to ensure that collective states are symmetrized with respect to the $\bar{D}_{4y}$ intrinsic symmetry group. The conservation of the body-fixed frame adds conditions on the octupole variables $\text{Im}(\alpha_{3\nu}) = 0$ during the collective motion. In brief, the symmetrization condition requires that each collective state as the eigensolution of the collective Hamiltonian of Eq. (3) has to be invariant with respect to the symmetrization group. Obtained in this way solutions are unique in the laboratory frame, and thus can be named physical states.

Let us also observe that the rotational Hamiltonian (5), by construction, contains, besides the constant term T_{00}, the

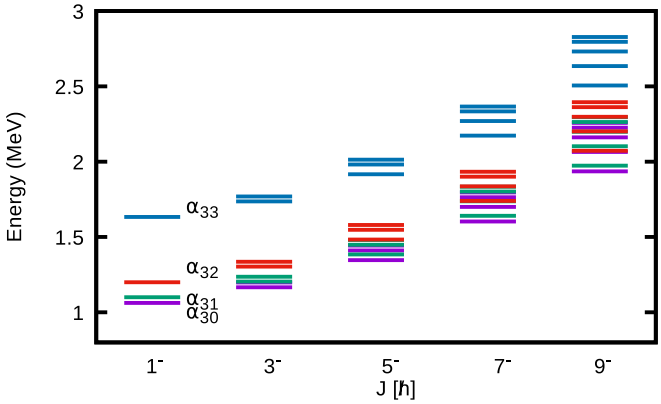

FIG. 5. The negative-parity states built on octupole axial and nonaxial one-phonon excitations in ^{156}Dy. Colors mark $(J+1)/2$ states with different κ numbers for given spin J.

components of angular-momentum operators of power two only, and, as a consequence, is time-reversal invariant. By the fact that the vibrational Hamiltonian term, defined in Sec. II A, is obviously invariant with regard to the time-reversal operation, one concludes that the full Hamiltonian keeps this symmetry.

In general, as written in Ref. [11], states with negative κ are linearly dependent on those with positive κ. This means that both are composed of identical (real) combinations of rotational basis functions (differing only by the sign of K) and therefore can be considered as mutual time-reversed states. Consequently, it is sufficient to solve the Hamiltonian eigenproblem within the basis-function subset with, e.g., $\kappa > 0$. Finally, each resulting eigenstate has to be treated as doubly degenerate.

Figures 6 and 7 present a distribution of rotational basis states of given K in the collective eigensolutions of spin J belonging to the ground-state band and the two above-discussed candidate bands based on α_{30} and α_{32} one-phonon excitations associated respectively with band 2 and band 4. Shown is only the probability for $K > 0$ quantum numbers since they

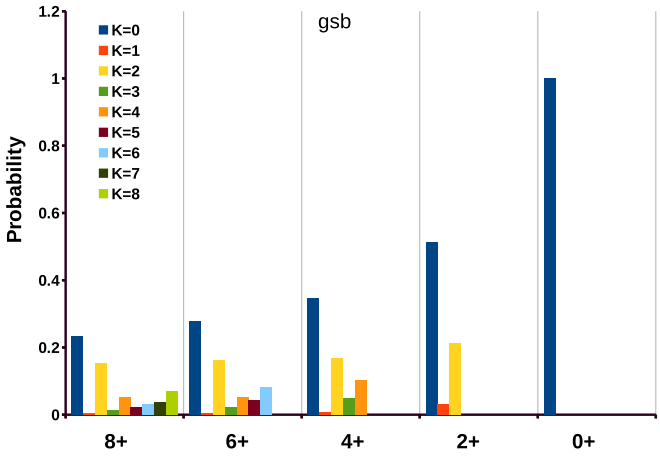

FIG. 6. The distribution of rotational basis states of given K for the ground-state band of the ^{156}Dy.

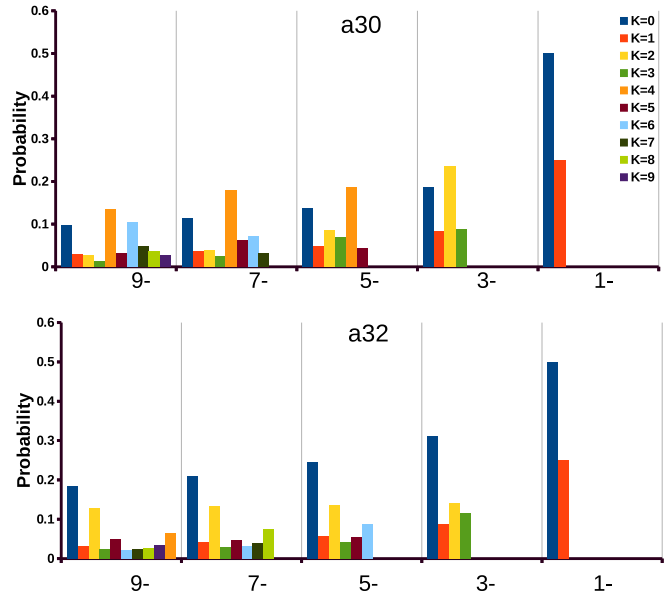

FIG. 7. Distribution of rotational basis states of given K for two model bands based on α_{30} and α_{32} one-phonon excitations of ^{156}Dy for odd-spin negative-parity-level scheme describing the experimental band 2.

are identical for $K < 0$. The ground-state sequence is mainly dominated by $K = 0$ and $K = 2$ components (Fig. 6). One observes that, in the axial-octupole band of Fig. 7, the largest rotational components are characterized by $K = 0$ and $K = 4$ while the second, nonaxial tetrahedral band, is characterized by components with $K = 0$ and $K = 2$.

When the even-spin negative-parity band is concerned, the K number mixing is presented in Fig. 8. Here, the main contributions have $K = 2$ and $K = 4$. This mixing pattern is different than for the odd-spin band, dominated by $K = 0$.

One therefore deduces that none of the theoretical bands considered characterized by one-phonon $\alpha_{3\nu}$ excitations has

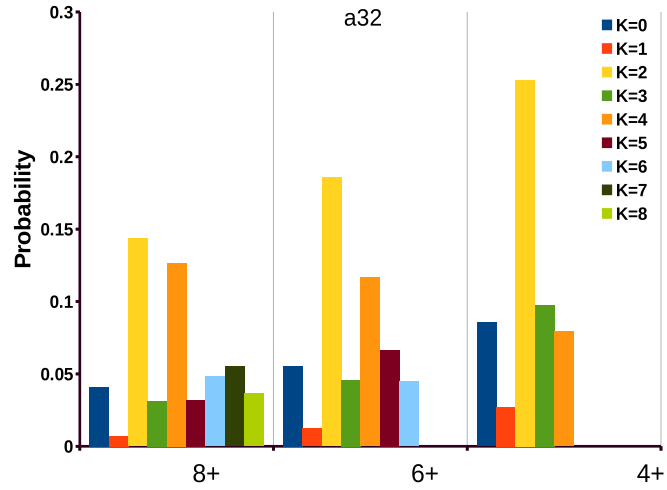

FIG. 8. Similar to Fig. 7 but for model band based on α_{32} one-phonon excitation as a candidate for even-spin negative-parity-level scheme of experimental band 4.

a well-fixed spin projection number K in the chosen intrinsic frame. Let us recall that the conditions imposed on quadrupoles, i.e., $\alpha_{21} = \alpha_{2-1} = 0$ and $\alpha_{22} = \alpha_{2\text{-}2}$, to define the body-fixed coordinate system are identical as in the Bohr–Hamiltonian model of, e.g., Ref. [14].

Seemingly, the mixing of the K numbers within a given octupole band is caused by a relatively high-order symmetrization group, $\bar{D}_{4y}$ which combines rotational basis states of different K within a given vibrational structure, as defined in Eq. (9). As demonstrated in Ref. [34], the use the most general complex space of all octupole variables $\alpha_{3\mu} \in \mathcal{C}$, instead of real ones exploited in this study, leads to the octahedral symmetrization group. As known from the studies of the quadrupole bands within the Bohr–Hamiltonian approach, this group, similar to the $\bar{D}_{4y}$ one, mixes, within a given state, the rotational contributions of different K as well.

As an exception, one can imagine an unrealistic collective model with the symmetrization group composed only of the rotations about the intrinsic OZ axis, which would keep the K number unchanged within the whole collective band. In addition, any group composed of C_{nz} rotations about an angle $2\pi/n$, where $n \in \mathcal{N}$, and being a subgroup of the SO(2), imposes the condition for variables $\alpha_{\lambda\rho}$ that ρ/n should be an integer number. This implies that, for $n \leqslant 3$, some deformations $\alpha_{2\mu}$ and $\alpha_{3\nu}$ are eliminated from the model or, for the case $n \geqslant 3$, only axial deformations $\alpha_{\lambda 0}$ are left. Another example of a nonphysical symmetrization group could be the C_{2y} group composed only of the rotation about the angle π with respect to the OY axis and the identity operation. It turns out that this particular would not mix the contributions with different K, either.

On the other hand, we investigated that any three realistic conditions imposed on the quadrupole and/or octupole variables to fix the intrinsic frame in unique way always lead to symmetrization groups possessing more than one rotation axis. One therefore deduces that the issue of K mixing within the vibrational-rotational collective bands is neither the effect of the presence of these limiting conditions on the variable space nor computational artifacts but should rather be treated as an imminent property of such bands.

C. Strength of $B(E\lambda)$ transitions

As mentioned at the end of Sec. III A, knowing only the energies of the band members, one is not unequivocally able to associate a given theoretical sequence of levels with the experimentally determined band. The study of the probabilities of the electric transitions is therefore obligatory to predict more faithfully the vibrational and rotational structures of these bands.

According to the experimental indications, the ground-state well in the ^{156}Dy nucleus is strongly quadrupole deformed. This means that, in the equilibrium state, octupole degrees of freedom are, in the first approximation, not excited. It implies that in the function (9) $\sum_{\rho=0}^{3} n_{3\rho} = 0$ whereas n_{20} and n_{22} values are assumed to be 0, 1, 2, 3. For the negative-parity states, on the contrary, $n_{20} = 0$ and $n_{22} = 0$, while in the octupole part of this function, $\sum_{\rho=0}^{3} n_{3\rho} = 1$ or 3. Due to the parity property, even-phonon numbers on the right-hand side of the previous condition are not permitted.

An essential problem is to fix the values of the model parameters. The first group of parameters are the shifts $\mathring{\alpha}_{2\mu}$ and $\mathring{\alpha}_{3\nu}$ in Eq. (9) for $\lambda = 2,3$ and $-\lambda \leqslant \mu \leqslant \lambda$. These parameters mean that all the basis functions (9) are centered over the potential-energy minimum in our six-dimensional deformation space, i.e., at the point $(\alpha_{20}, \alpha_{22}, \alpha_{30}, \alpha_{31}, \alpha_{32}, \alpha_{33}) = (0.25, 0.0, 0.0, 0.0, 0.0, 0.0)$.

The second group of basis parameters in function (9) is the so-called "widths," $\eta_{\lambda\mu}$. Certainly, for the incomplete basis set, the parameters $\eta_{\lambda\mu}$ are absolutely crucial. We have decided that the optimal values of these parameters should correspond to the minimal collective energy of the ground state with respect to all $\eta_{\lambda\mu}$, i.e., $E_{gs} = E_{gs}(\{\eta_{\lambda\mu}\}) = \min$.

As we see, both of these groups of parameters are determined by using clear criteria referring to the properties of the potential energy as a function of the deformation. None of these parameters has been adjusted to the experimental data; however, to get a better agreement of the energies of states with the measured values, some "fine tuning" of the moments of inertia of Eq. (8) in future studies would be necessary. In general, the reduced transition probability of the electric $E\lambda$ transition finally reads

$$B(E\lambda, J \to J') = \frac{\left|\langle J'\pi'\kappa' || \hat{Q}_{\lambda}^{(\mathrm{lab})} || J\pi\kappa \rangle\right|^2}{2J+1}, \qquad (11)$$

where J, π, and κ are the actual quantum numbers of the model, and $\hat{Q}_{\lambda}^{(\mathrm{lab})}$ is the transition operator of multipolarity λ defined in the laboratory frame. The latter are simulated by the multipole-moment operators with the constant proton density distribution and $R_0 = 1.2A^{1/3}$, as done, e.g., in Ref. [35].

Since, as mentioned above, in the case of the $\bar{D}_{4y}$ symmetrization group, K is not conserved within the band, one may in fact construct more than one band of collective states described by the same vibrational structure and different combinations of K. To assemble a band of theoretical Hamiltonian eigensolutions one has admitted that within this sequence the one-phonon vibrational structure is conserved and, in parallel, the intraband $B(E2)$ values have to lower monotonically with lowering spin. The strengths of the quadrupole $B(E2)$ matrix elements are determined both by the intrinsic vibrational (quadrupole moments) and rotational (appropriate Clebsch–Gordan coefficients) properties of the state.

The arguments presented here lead, in principle, to rather qualitative conclusions. We are aware of the fact that the model used is not able to perfectly reproduce the absolute values of energies E_γ (Table I) and transition probabilities $B(E1)$ and $B(E2)$ (Table II).

Nevertheless, the overall tendency of the $B(E1)/B(E2)$ ratio for the preselected sequences of states called theoretical bands as a function of spin, shown in parentheses in Figs. 3 and 4, can be directly extracted from the calculations. First, for the negative-parity bands based on one-phonon $\alpha_{3\mu}$ excitations, the lowering of the $B(E1)/B(E2)$ branching ratio with lowering spin, as discovered in the experiment, is visible in bands constructed on the α_{30} and α_{31} modes but, for the latter, this ratio is about one order of magnitude higher

than the experimental one of Ref. [10]. As also seen, in the so-called "tetrahedral" and nonaxial α_{33} bands this quantity is almost independent of spin. These facts may suggest that the experimental band, named in Ref. [10] band 2, may be most likely of axial octupole (α_{30}) character. Note also that the nonaxial α_{31} band efficiently competes with the latter.

The hypothesis that the vanishing of the intraband $B(E2)$ transitions below $J = 7^-$ state in the studied negative-parity band 2 of the ^{156}Dy nucleus can be provoked by the presence of the tetrahedral symmetry is apparently not supported by this model. The intraband $B(E2)$ values in the band built on the axial α_{30} mode are, in general, lower by approximately 40% than in the tetrahedral band, which is somehow in contradiction to early simplistic approaches proposed to identify the tetrahedral symmetry.

As commonly known, their values are predominantly determined by the quadrupole moment of the bandhead and the rotational structures of individual states in terms of the K-number distribution of the initial and final configurations. As discussed in Sec. II C, all octupole negative-parity bands, including the tetrahedral one, are constructed on top of the quadrupole deformed ground state; their quadrupole moments are practically identical. Therefore, the substantial variations in $B(E2)$ values between different model bands come from differences in their rotational structures.

Where the dipole $E1$ transitions is concerned, in the axial α_{30} and nonaxial α_{31} octupole bands, the $B(E1)$ reduced transition probabilities grow monotonically by an order of magnitude upon lowering the spin from 9^- to 1^- while in the tetrahedral band the spin is almost unchanged. Observe that, in all proposed odd-spin model bands the magnitude of $B(E1)$ vary between 10^{-4} to 10^{-3} W.u. while in the even-spin one, between 10^{-4} to 10^{-6} W.u.

Coming to the even-spin band 4 plotted in Fig. 4, the only theoretical candidate is constructed on the one-phonon tetrahedral excitation since its corresponding energy levels (Table I) and the electric transition probability $B(E2)/B(E1)$ ratios are the closest to the experimental data. The predicted $B(E2,8^- \to 6^-)/B(E1,8^- \to 8^+)$ and $B(E2,6^- \to 4^-)/B(E1,6^- \to 6^+)$, as seen, are too small by a factor of 6–7 compared with the experimental values. On the other hand, the ratios corresponding to other two α_{30} and α_{33} one-phonon excitations deviate even by two and more orders of magnitude which is why they cannot be considered as potential candidates to reproduce the experimental band 4.

Since all the results are obtained within a pure collective approach, the $E1$ transition operator is constructed from the tensor couplings of the quadrupole and octupole $(\alpha_{2\mu} \otimes \alpha_{3\nu})$ modes, treated as its *second-order contributions*. For more details see Ref. [21]. To be detailed, the *first-order contributions* to the $E1$ transition operator would be proportional to $\alpha_{10}, \alpha_{1\pm1}$ independent dipole deformations which are not considered in this work.

However, the presence of the $\alpha_{3\nu}$ variables introduce a shift of the center of mass of the nuclear surface with respect to the beginning of the coordinate system—a spurious effect which should certainly be eliminated from the transition dipole operator. To cure this drawback we determine the so-called *induced dipole deformations* as functions of independent variables $\alpha_{2\mu}$ and $\alpha_{3\nu}$ which, when inserted into expansion (1), translate the center of mass back to the beginning of the coordinate system.

The same induced α_1 variables play here the role of the first-order contributions in the dipole transition operator. Here we profit from the approximate property of the α_1-type deformations as being responsible for the center-of-mass motion. As mentioned in Ref. [21] and references therein, such a shift is always accompanied by a certain modification of the surface shape. The stronger the deformation α_1, the larger the change in the nuclear body.

Finally, notice that, defined in such a way, the transition operator does not, by construction, take into account the microscopic effect of charge-density variation with the surface curvature, known as the polarization effects. We are convinced that, for the discussion herein, low-lying collective configurations built in the ground-state well and characterized by fairly compact shapes, this kind of effect is supposed, in the first approximation, to be negligible. In contrast, as concluded in Ref. [21], effects related with the center-of-mass shift can change the $B(E1)$ estimates up to $\approx$40%.

IV. SUMMARY

The model discussed allows us to construct the positive- and negative-parity collective states based on $\alpha_{2\mu}$ and $\alpha_{3\nu}$ degrees of freedom. In ^{156}Dy are a number of measured collective bands, but our interest is focused only on band 2 and band 4 in which, as written in a very recent publication [10], structure is questionable.

The analysis of the theoretical ground-state and the negative-parity-model bands reveals their tendency to be slightly "squeezed" compared with experimental ones. This clearly is an indication that some "fine tuning" of the coupling constants of the rotational Hamiltonian, here obtained on the basis of the cranking moments of inertia and Eq. (8), is needed. Please note that these constants are determined at the ground-state point and are assumed to be constant during the vibrational motion. In other words, a mechanism of vibration-rotation coupling through the deformation-dependent moments of inertia is, at this stage, neglected. On the other hand, it is interesting and remarkable that the relative energies of the octupole states with respect to the states of the equilibrium band are reproduced in a satisfactory way within some 0.1 MeV, which may indicate a reasonable predictive ability of the model.

Every vibrational-rotational state characterized by a given type of excitation and the number of excited phonons that can occur in $J + 1$ configurations are described by a specific combinations of K numbers, which ensure the state to be symmetrized with respect to the symmetrization $\bar{D}_{4y}$ group. Usually half of these states are linearly dependent and thus are not used directly in numerical calculations. Excitations in α_{30}, α_{31}, and α_{32} are close each other in energy (within some 150 keV).

For the odd-spin negative-parity bands based on one-phonon excitations in a $\alpha_{3\mu}$ mode, the lowering of the $B(E2)/B(E1)$ ratio with lowering spin, as discovered in the experimental band 2, is seen in the case of bands built on α_{30} and α_{31} modes. The tetrahedrally and α_{33} excited bands give

this ratio slowly changing with spin. As already mentioned in Ref. [11], the $E2$ transitions are almost insensitive to changes of octupole deformation, thus the main contribution to the $B(E2)/B(E1)$ changes is due to dipole transitions. The value of $B(E1)$ probability gives the information about dipole moment Q_1 which, in here used approximation, is proportional to the tensor coupling $\alpha_{2\nu} \times \alpha_{3\mu}$ tensors. A more detailed study on that is done in Ref. [21]. Briefly, the stronger dipole transitions $B(E1)$ (or dipole moment Q_1) with lowering spin, the stronger effective octupole deformation of the collective band is then obtained. Otherwise, for bands built on α_{32} and α_{33} phonons, its octupole deformation is getting larger and larger with increasing spin.

Another interesting point is the issue that the quantum number K seems to be not conserved within the vibrational-rotational bands studied here. Each excited rotational state is constructed as the superposition of rotational contributions with different K values with amplitudes remarkably different from zero. As demonstrated, this is a consequence of the quite-high symmetrization group associated with our model. Nonetheless, the K-mixing amplitudes may, to some extent be model dependent.

ACKNOWLEDGMENTS

This work was supported by the COPIN-IN2P3 Polish–French Collaboration under Contract No. 04-113 and the Polish National Science Centre under Contract No. 2013/08/M/ST2/00257 (LEA COPIGAL) and by Contract No. 2013/11/B/ST2/04087.

[1] S. G. Rohoziński, Phys. Rev. C **56**, 165 (1997).
[2] J. Dudek, A. Góźdź, and N. Schunck, Acta Phys. Pol. B **34**, 2491 (2003).
[3] J. Dudek, A. Góźdź, N. Schunck, and M. Miśkiewicz, Phys. Rev. Lett. **88**, 252502 (2002).
[4] J. Dudek, J. Dobaczewski, N. Dubray, A. Góźdź, V. Pangon, and N. Schunck, Int. J. Mod. Phys. E **16**, 516 (2007).
[5] J. Dudek, A. Góźdź, D. Curien, V. Pangon, and N. Schunck, Acta Phys. Pol. B **38**, 1389 (2007).
[6] S. G. Rohoziński, Rep. Prog. Phys. **51**, 541 (1988).
[7] P. A. Butler and W. Nazarewicz, Rev. Mod. Phys. **68**, 349 (1996).
[8] N. Minkov and P. M. Walker, Eur. Phys. J. A **48**, 80 (2012); Phys. Scr. **89**, 054021 (2014); P. M. Walker and N. Minkov, Phys. Lett. B **694**, 119 (2010).
[9] L. Bonneau, N. Minkov, Dao Duy Duc, P. Quentin, and J. Bartel, Phys. Rev. C **91**, 054307 (2015).
[10] D. J. Hartley, L. L. Ridinger, R. V. F. Janssens, S. N. T. Majola *et al.*, Phys. Rev. C **95**, 014321 (2017).
[11] A. Dobrowolski, K. Mazurek, and A. Góźdź, Phys. Rev. C **94**, 054322 (2016).
[12] W. Nazarewicz, P. Olanders, I. Ragnarsson, J. Dudek, G. A. Leander, P. Möller, and E. Ruchowska, Nucl. Phys. A **429**, 269 (1984).
[13] W. Nazarewicz, J. Dudek, R. Bengtsson, T. Bengtsson, and I. Ragnarsson, Nucl. Phys. A **435**, 397 (1985).
[14] L. Próchniak and S. G. Rohoziński, J. Phys. G **36**, 123101 (2009).
[15] P. G. Bizzeti and A. M. Bizzeti-Sona, Phys. Rev. C **70**, 064319 (2004); **77**, 024320 (2008).
[16] J. Engel and F. Iachello, Nucl. Phys. A **472**, 61 (1987).
[17] D. Bonatsos, D. Lenis, N. Minkov, D. Petrellis, and P. Yotov, Phys. Rev. C **71**, 064309 (2005).
[18] T. M. Shneidman, G. G. Adamian, N. V. Antonenko, R. V. Jolos, and S.-G. Zhou, Phys. Rev. C **92**, 034302 (2015).
[19] S. Ćwiok, J. Dudek, W. Nazarewicz, J. Skalski, and T. Werner, Comput. Phys. Commun. **46**, 379 (1987).
[20] D. R. Inglis, Phys. Rev. **96**, 1059 (1954); **103**, 1786 (1956); S. T. Balyeav, Nucl. Phys. **24**, 322 (1961).
[21] A. Dobrowolski, A. Góźdź, and K. Mazurek, Acta Phys. Pol., B **48**, 565 (2017).
[22] R. D. Woods and D. S. Saxon, Phys. Rev. **95**, 577 (1954).
[23] N. Dubray, Ph.D. thesis, Université de Louis Pasteur de Strasbourg, 2005 (unpublished).
[24] J. Dudek, A. Góźdź and D. Rosły, Acta Phys. Pol. B **32**, 2625 (2001).
[25] M. Miśkiewicz, A. Góźdź, and J. Dudek, Int. J. Mod. Phys. E **13**, 127 (2004).
[26] J. Dudek, K. Mazurek, and B. Nerlo-Pomorska, Int. J. Mod. Phys. E **13**, 117 (2004).
[27] K. Mazurek and J. Dudek, AIP Conf. Proc. **802**, 153 (2005).
[28] K. Pomorski and J. Dudek, Phys. Rev. C **67**, 044316 (2003).
[29] J. Dudek, K. Pomorski, N. Schunck, and N. Dubray, Eur. Phys. J. A **20**, 15 (2003).
[30] V. M. Strutinsky, Nucl. Phys. A **122**, 1 (1968).
[31] D. R. Bes and Z. Szymanski, Nucl. Phys. **28**, 42 (1963).
[32] M. Bolstreli, E. O. Fiset, J. R. Nix, and J. L. Norton, Phys. Rev. C **5**, 1050 (1972).
[33] H. J. Krappe, J. R. Nix, and A. J. Sierk, Phys. Rev. C **20**, 992 (1979).
[34] A. Góźdź, A. Szulerecka, A. Dobrowolski, and J. Dudek, Int. J. Mod. Phys. E **20**, 199 (2011).
[35] J. M. Eisberg and W. Greiner, *Nuclear Models: Collective and Single Particle Phenomena* (North-Holland, Amsterdam, 1987).